

# The atomic and electronic structure of amorphous silicon nitride

F. Alvarez and A. A. Valladares\*

*Instituto de Investigaciones en Materiales, UNAM,  
Apartado Postal 70-360, 04510, México D.F.,*

*\* e-mail: valladar@servidor.unam.mx*

Recibido el 20 de marzo de 2002; aceptado el 2 de julio de 2002

Using a novel approach to the *ab initio* generation of random networks we constructed two nearly stoichiometric samples of amorphous silicon nitride with the same content  $x=1.29$ . The two 64-atom periodically-continued cubic diamond-like cells contain 28 silicons and 36 nitrogens randomly substituted, and were amorphized with a 6 fs time step by heating them to just below their melting temperature with a Harris-functional based, molecular dynamics code in the LDA approximation. The averaged total radial distribution function (RDF) obtained is compared with some existing Tersoff-like potential simulations and with experiment; ours agree with experiment. All the partial radial features are calculated and the composition of the second peak also agrees with experiment. The electronic structure is calculated and the optical gaps obtained using both a HOMO-LUMO approach and the Tauc-like procedure developed recently that gives reasonable gaps.

**Keywords:** Amorphous semiconductors; radial distribution functions; amorphous silicon nitride.

Utilizando un enfoque innovador *ab initio* para la generación de redes estocásticas, hemos construido dos muestras casi estequiométricas de nitruro de silicio amorfo con el mismo contenido  $x = 1.29$ . Las dos celdas de 64 átomos, cúbicas tipo diamante, con condiciones periódicas, contienen 28 silicios y 36 nitrógenos substituidos al azar y fueron amorfizadas con un *time step* de 6 fs calentándolas hasta una temperatura justo abajo de la de fusión, con un código de dinámica molecular, en la aproximación LDA, basado en la funcional de Harris. La función de distribución radial (RDF) total obtenida se compara con simulaciones clásicas que utilizan potenciales tipo Tersoff y con el experimento; las nuestras concuerdan con el experimento. Se calculan todas las características radiales parciales; la composición del segundo pico concuerda también con el experimento. La estructura electrónica también se calcula y las brechas ópticas obtenidas, utilizando tanto un enfoque HOMO-LUMO, como el procedimiento tipo Tauc que desarrolláramos recientemente, dan brechas razonables.

**Descriptores:** Semiconductores amorfos; funciones de distribución radial; nitruro de silicio amorfo.

PACS: 71.23.Cq; 71.15.Pd; 71.55.Jv

## 1. Introduction

Silicon nitride ( $\text{Si}_3\text{N}_4$  or  $\text{SiN}_{1.33}$ ) is a very important ceramic due to its chemical, mechanical and electronic properties. It is chemically inert and due to its superior mechanical properties at high temperatures has been used in engine components and cutting tools [1, 2]. Also, due to its high dielectric constant and large electronic gap it has been used in microelectronic devices [3]. Amorphous silicon nitride has all these properties plus isotropy, due to its random nature and therefore it is also a very useful material. However, characterization of the atomic and electronic structure of the amorphous phase has proven to be a very difficult task.

There are two main lines that have been followed in studying amorphous solids. The first line is the use of clusters to simulate the structure of the materials; the advantage is that one can construct clusters with specific arrangements to closely resemble the structures found in random solids; the disadvantage is that clusters intrinsically have boundary effects not found in real solids. The second line is the use of supercells that are amorphized and repeated periodically to simulate the extended solid, but in general the resulting structures can not be controlled. The calculational efforts have evolved along two avenues. On the one hand there is the classical modeling of interatomic potentials that have permitted the study of large cells of pure elements, with tens of thousands of atoms. On the other hand there are the quantum methods, parameterized and *ab initio*, that aim at describ-

ing the systems without recourse to classical potentials that, by necessity, leave out interactions and correlations proper to the quantum entities that form the systems. However, the *ab initio* techniques are the way to go whenever good qualitative universal results are required and whenever new parameters are needed for the above-mentioned approximate techniques. Their shortcoming are the large computer resources needed to deal with cells of several hundred atoms that would make the description of the electronic and atomic structures of amorphous semiconductors more inclusive.

Recent work has demonstrated, nevertheless, that the application of *ab initio* techniques to the generation of random networks of C, Si, Ge and  $\text{SiN}_{1.29}$  [4] and *a*-Si:H, [5] using only 64-silicon atom cells, plus hydrogens, is reasonable. No doubt, being able to handle a sample with more than 64 atoms would allow us to study non-microscopic defects like large voids, for example, but the results found are encouraging. We believe the success of our method is due to two factors: first we amorphize the cell at temperatures just below its melting point; in this manner we avoid the generation of undesirable structures that are generated when samples are liquified first and solidified next. Second, we use a quantum code based on the Harris functional that incorporates “quantum” forces as derivatives of the energy in the Harris functional and is less demanding than the self consistent methods associated to the Kohn-Sham technique. It is known [6] that the melting temperature of *a*-Si is 250° C lower than the melting temperature of *c*-Si and therefore we expect to be above

the melting temperatures of the respective amorphous phases by staying just below the melting temperatures of the crystalline counterparts.

It is clear that, in principle, a full theoretical description of the properties of an amorphous solid depends on a complete knowledge of the atomic structure. However, for these solids there are an infinite number of possible structures and the best we can do to characterize their atomic arrangement is to use the radial distribution function (RDF), also known as the pair distribution function. Defined as  $4\pi r^2 \rho(r) dr$ , where  $\rho(r)$  is the density of particles at point  $r$ , the RDF gives the average number of pairs of atoms separated by a distance between  $r$  and  $r+dr$ . A given structure generates a well defined RDF but a given RDF corresponds to many atomic structures; that is, there is not a one to one correspondence between a given structure and its corresponding RDF.

The experimental and theoretical activity prior to 1990 is well documented in a paper by Robertson where pertinent references can be found [8]. On the experimental side, as early as 1976, Voskoboynikov *et al.* [9] studied some RDFs and optical gaps of silicon-rich silicon-nitrogen films as a function of the gas ratio. It was then observed that the gaps increased as a function of the nitrogen content; the films seemed to contain hydrogen and large clusters of silicon. Their optical absorption curves already indicated pronounced tails for nitrogen rich samples. Experimental radial distribution functions are scarce [10] and only total ones for the stoichiometric amorphous composition exist [11]. A gaussian-based decomposition of the second peak of the total RDF into its partial contributions is carried out by Misawa *et al.* [12].

Electronic structure studies of  $a\text{-SiN}_x$ , in the range  $0 \leq x < 2$ , were performed by Kärcher *et al.* [13] using X-ray photoelectron spectroscopy where the valence band was thoroughly analyzed and the Si-N bonding studied. It has now been established that the optical gap of  $a\text{-SiN}_x\text{:H}$  increases as  $x$  increases, slowly at first, and close to the stoichiometric compound,  $x = 4/3 = 1.33$ , it attains its largest values [10]. There are some experimental results for the optical gaps of non-hydrogenated amorphous silicon-nitrogen alloys reported by Sasaki *et al.* [14] and Davis *et al.* [10], and the conclusions are similar.

Ordejón and Ynduráin [15] do non-parameterized calculations of  $a\text{-SiN}_x$  where the equilibrium positions of Si and N atoms in clusters are ported to the alloy network constructed *ad hoc*. They obtain a wealth of information including optical gaps, but no RDFs; however, tetrahedral coordination of the silicon atoms and threefold planar coordination of the nitrogen atoms is *assumed* throughout, with interatomic distances of 2.33 Å for Si-Si and 1.74-1.76 Å for Si-N; compare to the crystalline values: 2.352 Å for Si-Si and 1.71-1.76 Å for Si-N [16]. A general characteristic of practically all calculations/simulations done up to date is that gap states, when considered, are introduced either by hand, progressively replacing Si by N, or by the algorithms that generate the random networks, *unlike* the procedure reported in our work. Recent semiempirical classical molecular dynamics simula-

tions by de Brito *et al.* [17] produced total RDFs that are the subject of comparison with ours.

In what follows we present the first *ab initio* generated random networks for two structures of amorphous silicon nitride.

## 2. Method

Our two amorphous samples of silicon nitride were generated using a new approach that leads to structures with realistic partial and total RDFs and with realistic optical gaps as well [18]. We use *Fast Structure\_SimAnn* [20], (*Fast* for short) a DFT molecular dynamics code that is based on the Harris functional [21], and optimization techniques with a fast force generator to allow simulated annealing/molecular-dynamics studies with quantum force calculations [22]. We use the LDA parameterization due to Vosko, Wilk and Nussair [23] throughout. The core is taken as full which means that an all electron calculation is carried out, and a minimal basis set of atomic orbitals was chosen with a cutoff radius of 5 Å for the amorphization and 3 Å for the optimization. In order to better simulate the dynamical processes that occur in the amorphisation a time step of 6 fs was used. The forces are calculated using rigorous formal derivatives of the expression for the energy in the Harris functional, as discussed by Lin and Harris [24]. For each atom, one function is used to represent the core part of the density and one to represent the valence density. The type of orbital basis in *Fast* are: *minimal* (the orbital basis consists of atomic orbitals occupied in the neutral atom; *sp*-valence type); *standard* (broadly equivalent to a DN basis set; *i. e.*, to a Double Numeric basis set) and *enhanced* (broadly equivalent to a DNP basis set; *i. e.*, to a Double Numeric set together with Polarization functions). The evaluation of the 3-center integrals that contribute to the matrix elements in the one-particle Schrodinger equation is the time-limiting feature of *Fast* and each is performed using the weight-function method of Delley [25].

To test the adequacy of the amorphous structures obtained with *Fast* we used it to calculate the size of the crystalline cell of  $\beta\text{-Si}_3\text{N}_4$  that minimizes the energy at the  $\Gamma$ -point using orbital basis of the *minimal* type. Figure 1. shows the results of such calculation. The experimental crystalline volumen is given by 145.920 Å<sup>3</sup>, [26] whereas the calculated volumen is 146.797 Å<sup>3</sup>; a deviation of 0.6%. This indicates that *Fast* is adequate to deal with silicon nitride.

It has become increasingly clear that quenching from a melt generates undesirable structures, so we took a different path [4]. We amorphized the crystalline diamond-like structures with a total of 64 atoms in the cell, 28 silicons and 36 randomly substituted nitrogens, Fig. 2a by heating them up, linearly, from room temperature to 2162 K, just below their melting point, and then cooling them down to 0 K. The heating/cooling rate for the stoichiometric cells was  $3.11 \times 10^{15}$  K/s. Using cells with 27 silicons and 37 nitrogens would have given a content of 1.37, above 1.33 the stoichiometric one. The atoms were allowed to move within each cell whose volume was determined by the density  $3.115 \text{ g cm}^{-3}$

taken from the experimental results of Guraya *et al.* [10], and periodic boundary conditions were always used. Once this first stage was completed, *Fast* was used to subject each cell to annealing cycles at 300 K with intermediate quenches down to 0 K. Finally the samples were energy-optimized to make sure the final structures would have local energy minima. One final random structure is shown in Fig. 2b. It has become increasingly clear that quenching from a melt generates undesirable structures, so we took a different path [4]. We amorphized the crystalline diamond-like structures with a total of 64 atoms in the cell, 28 silicons and 36 randomly substituted nitrogens, Fig. 2a by heating them up, linearly, from room temperature to 2162 K, just below their melting point, and then cooling them down to 0 K. The heating/cooling rate for the stoichiometric cells was  $3.11 \times 10^{15}$  K/s. Using cells with 27 silicons and 37 nitrogens would have given a content of 1.37, above 1.33 the stoichiometric one. The atoms were allowed to move within each cell whose volume was determined by the density  $3.115 \text{ g cm}^{-3}$  taken from the experimental results of Guraya *et al.*, [10] and periodic boundary conditions were always used. Once this first stage was completed, *Fast* was used to subject each cell to annealing cycles at 300 K with intermediate quenches down to 0 K. Finally the samples were energy-optimized to make sure the final structures would have local energy minima. One final random structure is shown in Fig. 2b.

Both the cutoff radius [27] and the completeness of the orbital set play a role in simulations. In a previous work [18] we have established that the best combination for these alloys is to use the minimal basis set throughout with a cutoff radius of 5 Å for the amorphization and 3 Å for the optimization.

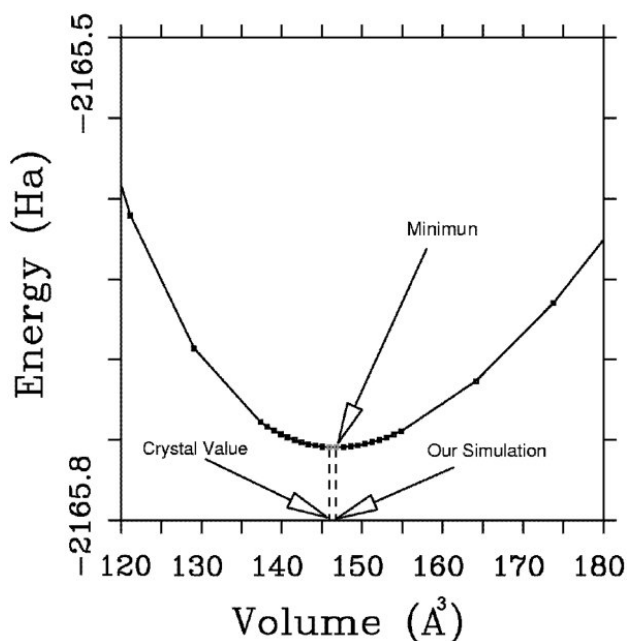


FIGURE 1. Energy vs volume for crystalline  $\beta$ - $\text{Si}_3\text{N}_4$  obtained with *Fast* and experimental values taken from Wild *et al.* [26]. The volumes agree to within 0.6%.

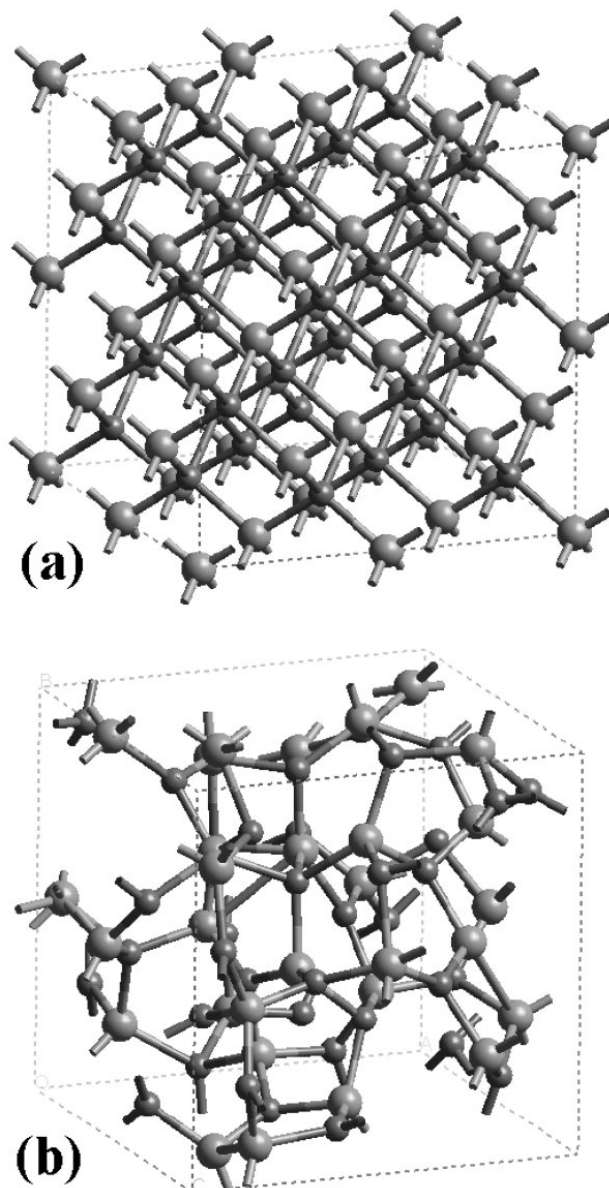


FIGURE 2. (a) Initial (crystalline supercell), and (b) final (amorphous supercell) structures for silicon nitride.

### 3. Results and discussion

Our objective is to generate realistic amorphous structures of amorphous silicon nitride and not, in any way, to mimic the experimental processes used to produce these alloys. Since the atomic topology determines the electronic properties of the amorphous samples any understanding of the RDFs and the atomic distribution in the random networks is relevant for the characterization of the electronic and optical properties of amorphous materials.

The total RDFs for the total and partial RDFs for each of the two silicon nitride supercells are calculated and are then averaged. The averaged total and partial RDFs for the stoichiometric content are given in Fig. 3. In the partial features

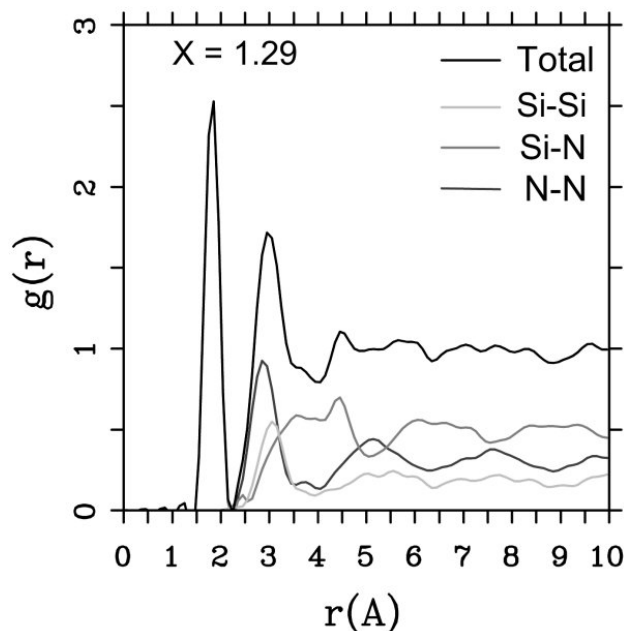


FIGURE 3. Total and partial RDFs for stoichiometric silicon nitride. The Si-Si, Si-N and N-N partials can be observed. Total and partial RDFs for stoichiometric silicon nitride. The Si-Si, Si-N and N-N partials can be observed.

one can see the size of the Si-Si, N-N and Si-N peaks and their influence on the total RDF. These curves are plotted as they are, *i.e.*, as the number of atoms at a certain radial distance from a given one, normalized to the density of the bulk material.

Figure 4. shows the comparison of our results for silicon nitride with the experimental ones [11] and also the comparison of de Britos classical simulations with experiment [11]. It can be seen that our work agrees very well with experiment. A very stringent test for our method is the composition of the second peak of the total RDF obtained from the simulation and the experimentally 'guessed' composition [12]. This is given in Fig. 5. where it can be observed that our simulation not only agrees with experiment, but improves on it since it reflects the real structure of this peak due to the fact that we *do not* assume a gaussian shape, as experimentalists do. It can be observed that the second peak is formed by the second neighbor contributions of mainly the N-N and Si-Si partials and to a lesser extent by the Si-N partial. Our simulation also predicts that the third peak is essentially due to the Si-N partial with a small contribution from the N-N partial, Fig. 3.; unfortunately there are no experimental findings for comparison.

In Fig. 6. we present the density of states (DOS) curves calculated with *Fast* at the  $\Gamma$  point, and an enlargement near the gap region. It can be seen that there exist gap states that are the result of the dangling, floating or strained bonds in the amorphous material. If we look at the highest occupied molecular orbital (HOMO) and the lowest unoccupied molecular orbital (LUMO) we can define a gap as the LUMO-HOMO, that is, as the energy difference between the LUMO

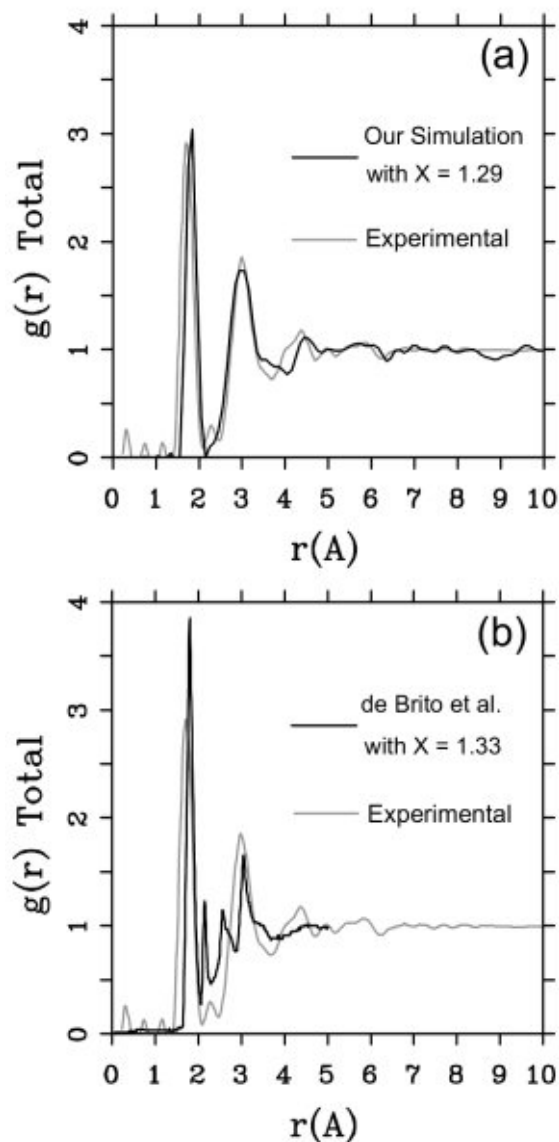


FIGURE 4. Total RDFs for the stoichiometric samples. (a) Comparison of our simulations with experiment [11]. (b) Comparison of de Brito's simulations with experiment [11].

and the HOMO, and the value obtained is 3.5 eV, small compared to the experimentally reported ones. That is why we developed a novel approach [18] to the calculation of the optical gaps along the lines of the Tauc method, popular among the experimentalist. In brief, one characteristic feature of optical absorption in amorphous semiconductors is that certain selection rules, which apply to optically induced transitions in crystalline materials, are relaxed. For interband absorption the following assumptions are commonly made [19]:

(a) The matrix elements for the electronic transitions are constant over the range of photon energies of interest and are given by  $D = \pi(a/\Omega)^{1/2}$ , where  $a$  is the average lattice spacing and  $\Omega$  is the volume of the specimen [19].

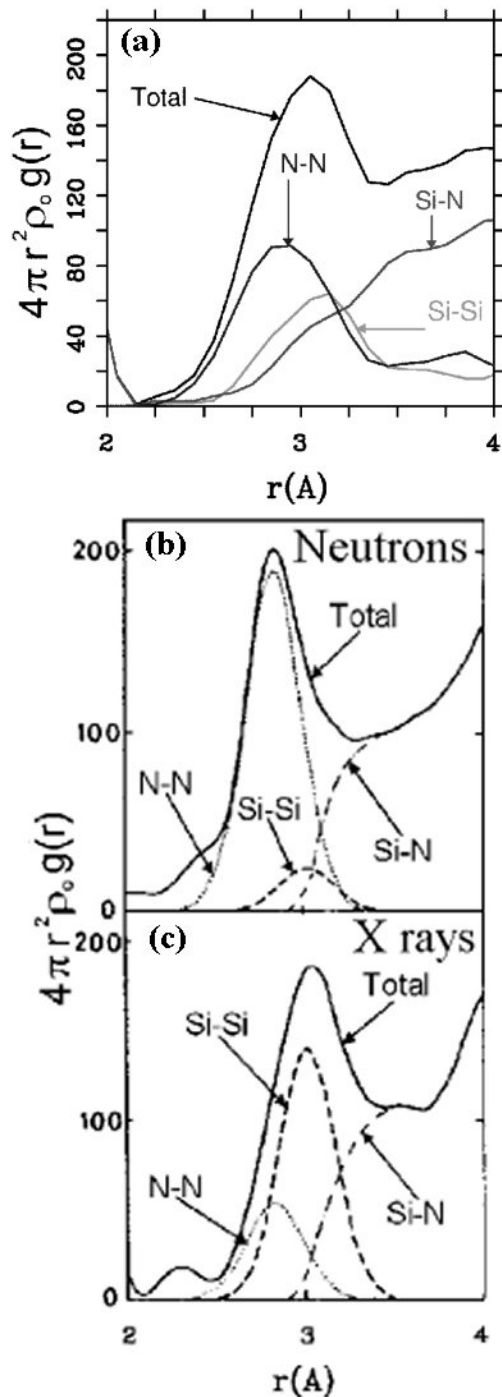


FIGURE 5. Comparison of the (a) simulated, (b) X-Ray determined and (c) neutron-determined experimental results for the second peak of silicon nitride; the agreement is excellent. Our results show that the Si-N partials are important.

(b) The  $k$ -conservation selection rule is relaxed. Under these conditions, the optical absorption coefficient  $\alpha$  for interband transitions is given by

$$\alpha = \frac{8\pi^4 e^2 \hbar^2 a}{n_o c m^2 \omega} \int N_V(E) N_C(E + \hbar\omega) dE$$

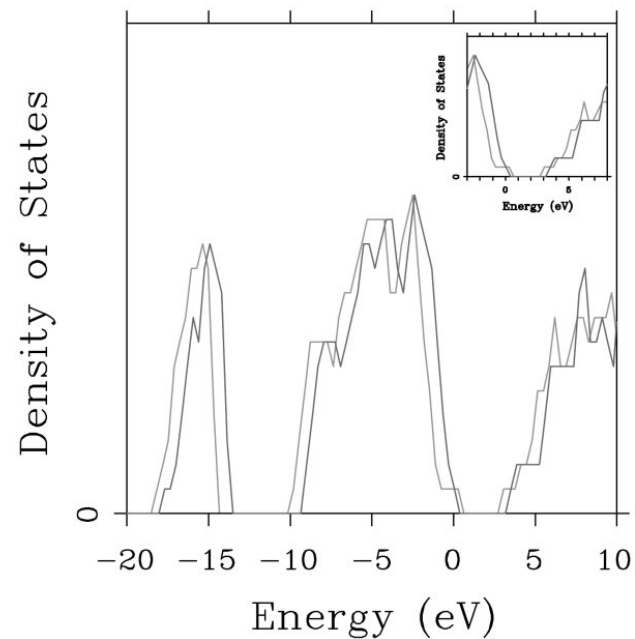


FIGURE 6. Density of states for the two samples of silicon nitride obtained at the  $\Gamma$  point. The insert shows a blow up of the gap region where gap states can be observed.

where the integration is over all pairs of states in the valence and conduction bands separated by an energy  $\hbar\omega$  [19].  $n_o$  is the refractive index.

For amorphous tetravalent semiconductors this leads to the well known relationship  $\sqrt{\alpha(\omega)\hbar\omega} = \text{const.}(\hbar\omega - E_0)$  obtained by Tauc [7] under the assumption of parabolic bands, formula that has been used extensively by experimentalists to obtain the optical gap  $E_0$  by plotting  $\sqrt{\alpha(\omega)\hbar\omega}$  vs  $(\hbar\omega - E_0)$ . Since  $\alpha$  is proportional to the fraction of energy lost by the wave on passing through the material this implies that it is proportional to the number of electronic transitions from the valence to the conduction band,  $N_t(\hbar\omega)$ . So plotting  $\sqrt{N_t(\hbar\omega)\hbar\omega}$  instead of  $\sqrt{\alpha(\omega)\hbar\omega}$  should give the same type of behavior as experimentally observed although with a different slope; however, the intersection with the horizontal  $\hbar\omega$  axis, the optical gap  $E_0$ , remains unaltered. This is precisely what we do: we look at the intersection of the linear fit to the  $\sqrt{N_t(\hbar\omega)\hbar\omega}$  data to find the optical gap. When this approach is applied to amorphous silicon nitride, the obtained average result 4.95 eV is more along the lines of the gap values reported experimentally [18].

#### 4. Conclusions

We have generated random networks for silicon nitride using the newly developed thermal procedure [4, 5] and an *ab initio* approach based on the Harris functional. Our simulated radial distribution functions agree very well with experiment. The total RDF for amorphous silicon nitride agrees very well with the only existing experimental result. The first prominent peak in this RDF is due to Si-N and an analysis

of the second peak indicates that N-N, Si-Si and Si-N contribute to it, in agreement with experiment. We also predict the structure of the third peak as being due mainly to the Si-N contribution, with a small contribution from the N-N; no experimental results exist for comparison. The electronic structure of amorphous silicon nitride is also presented and analyzed from the view point of HOMO-LUMO and also using the novel Tauc-like procedure. [18] We find gaps comparable to the experimental ones when the Tauc-like approach is used, and smaller values when the HOMO-LUMO approach is applied, as expected, since the HOMO-LUMO approach is sensitive to gap states.

Our method, being *ab initio*, is of wider applicability than classical or semiempirical ones and should be relevant for the understanding of the physics of amorphous covalent materials.

## Acknowledgments

A.A.V. thanks DGAPA-UNAM for financing Project IN101798 and IN100500. FA thanks CONACyT for supporting his PhD studies. This work was carried out on an Origin 2000 computer provided by DGSCA, UNAM.

1. R.N. Katz, *Science* **208** (1980) 841.
2. A.Y. Liu and M.L. Cohen, *Phys. Rev. B* **41** (1990) 10727.
3. M.J. Powell, B.C. Easton and O.F. Hill, *Appl. Phys. Lett.* **38** (1981) 794.
4. F. Alvarez, C.C. Díaz, Ariel A. Valladares and R.M. Valladares, *Phys. Rev. B* **65** (2002) 113108.
5. A.A. Valladares, F. Alvarez, Z. Liu, J. Sticht and J. Harris, *Eur. Phys. J. B* **22** (2001) 443.
6. J.M. Poate in *Electronic Materials. A New Era in Materials Science*, edited by J.R. Chelikowsky and A. Franciosi (Springer-Verlag, Berlin, Heidelberg, 1991), p. 323.
7. J. Tauc, in *Optical properties of solids*, edited by F. Abelès, (North Holland, Amsterdam, 1970).
8. J. Robertson, *Philos. Mag. B* **63** (1991) 47.
9. V.V. Voskoboynikov, V.A. Gritsenko, N.D. Dikovskaya, B.N. Saitsev, K.P. Mogilnicov, V.M. Osadchii, S.P. Sinitsa and F.L. Edelman, *Thin Solid Films* **32** (1976) 339.
10. S. Hasegawa, M. Matuura and Y. Kurata, *Appl. Phys. Lett.* **49** (1986) 1272; E.A. Davis, N. Piggins and S.C. Bayliss, *J. Phys. C* **20** (1987) 4415; M.M. Guraya, H. Ascolani, G. Zampieri, J.I. Cisneros, J.H. Dias da Silva and M.P. Cantão, *Phys. Rev. B* **42** (1990) 5677; G. Santana and A. Morales-Acevedo, *Solar Energy Materials & Solar Cells* **60** (2000) 135.
11. T. Aiyama, T. Fukunaga, K. Niihara, T. Hirai and K. Suzuki, *J. Non-Cryst. Solids* **33** (1979) 131; M. Misawa, T. Fukunaga, K. Niihara, T. Hirai and K. Suzuki, *J. Non-Cryst. Solids* **34** (1979) 313; T. Fukunaga, T. Goto, M. Misawa, T. Hirai and K. Suzuki, *J. Non-Cryst. Solids* **95 & 96** (1987) 1119.
12. M. Misawa, T. Fukunaga, K. Niihara, T. Hirai and K. Susuki, *J. Non-Cryst. Solids* **34** (1979) 313.
13. R. Kärcher, L. Ley and R.L. Johnson, *Phys. Rev. B* **30** (1984) 1896.
14. G. Sasaki, M. Kondo, S. Fujita and A. Sasaki, *Jpn. J. Appl. Phys.* **21** (1982) 1394.
15. P. Ordejón and F. Ynduráin, *J. Non-Cryst. Solids* **137&138** (1991) 891.
16. O. Borgen and H.M. Seip, *Acta Chem. Scand.* **15** (1961) 1789.
17. F. de Brito Mota, J.F. Justo and A. Fazzio, *Phys. Rev. B* **58** (1998) 8323; F. de Brito Mota, J.F. Justo and A. Fazzio, *Int. J. Quantum Chem.* **70** (1998) 973; F. de Brito Mota, J.F. Justo and A. Fazzio, *J. Appl. Phys.* **86** (1999) 1843; J.F. Justo, F. de Brito Mota and A. Fazzio, *Multiscale Modelling of Materials. Symposium, Mater. Res. Soc.* (1999) p. 555.
18. Fernando Alvarez and Ariel A. Valladares, *Appl. Phys. Lett.* **80** (2002) 58.
19. N.F. Mott and E.A. Davis, *Electronic processes in non-crystalline materials* (Oxford University Press, 1971) p. 238.
20. *FastStructure\_SimAnn, User Guide*, Release 4.0.0 (San Diego, Molecular Simulations, Inc., September 1996).
21. J. Harris, *Phys. Rev. B* **31** (1985) 1770.
22. Xiao-Ping Li, J. Andzelm, J. Harris and A.M. Chaka, Chapter 26 in *Chemical Applications of Density-Functional Theory*, Eds. B.B. Laird, R.B. Ross and T. Ziegler (American Chemical Society, Washington, DC, 1996).
23. S.H. Vosko, L. Wilk and M. Nusair, *Can. J. Phys.* **58**, (1980) 1200.
24. Z. Lin and J. Harris, *J. Phys. Condens. Matter* **5** (1992) 1055.
25. B. Delley, *J. Chem. Phys.* **92** (1990) 508.
26. S. Wild, P. Grieseson and K.H. Jack, *The crystal structure of alpha and beta silicon and germanium nitrides*. *Special Ceramics* 385 (1972).
27. O.F. Sankey and D.J. Niklewsky, *Phys Rev. B* **40** (1989) 3979.